Supporting Information

Facile synthesis of multi-resonance ultra-pure-green TADF emitters based on bridged diarylamine derivatives for efficient OLEDs with narrow emission

Guanting Liu[1], Hisahiro Sasabe[1,2,3], Kengo Kumada[1], Amane Matsunaga[1], Hiroshi Katagiri[1,2,3] and Junji Kido[1,2,3]**

[1]Department of Organic Materials Science, Graduate School of Organic Materials Science, Yamagata University, 4-3-16 Jonan, Yonezawa, Yamagata 992-8510, Japan, [2]Research Center for Organic Electronics (ROEL), Yamagata University, 4-3-16 Jonan, Yonezawa, Yamagata 992-8510, Japan, [3]Frontier Center for Organic Materials (FROM), Yamagata University, 4-3-16 Jonan, Yonezawa, Yamagata 992-8510 (Japan)

E-mail: (h-sasabe@yz.yamagata-u.ac.jp, kid@yz.yamagata-u.ac.jp)

General Considerations:

Quantum chemical calculations were performed using the hybrid density functional theory (DFT) functional Becke and Hartree-Fock exchange and Lee Yang and Parr correlation (B3LYP) as implemented by the Gaussian 09 program packages[1]. The molecular structure optimizations were performed at the B3LYP 6-31G(d) level. The E_S and E_T values were obtained from time-dependent (TD)-DFT calculation at the B3LYP 6-31G(d). ^{1}H NMR, ^{13}C and ^{11}B NMR spectra were recorded on JEOL 600 (600 MHz). Mass spectrum were obtained using a Waters SQD2 mass spectrometer with atmospheric pressure solid analysis probe (ASAP). TGA was undertaken using a SEIKO EXSTAR 6000 TG/DTA 6200 unit under nitrogen atmosphere at a heating rate of 10 °C min^{-1}. UV–vis spectra was measured using a Shimadzu UV-2600 UV–vis spectrophotometer. Photoluminescence spectra were measured using a FluoroMax^{-2} (Jobin-Yvon-Spex) luminescence spectrometer. The I_p was determined by a PYS under the vacuum (=10^{-3} Pa). Transient PL decay curves and time resolved photoluminescence spectra of solid film were measured by using a streak camera (C4334 from Hamamatsu Photonics) at 7 K and 300 K. PL decay time of dilute solution was detected using a Hamamatsu C11367 Quantaurus-Tau fluorescence lifetime spectrometer with an excitation wavelength of 350 nm. The temperature dependence of PL decay time was measured using a liquid nitrogen cryostat system (UNISOKU CoolSpeK). Photoluminescence quantum yield of **DMAc-BN** and **PXZ-BN** were measured using a Hamamatsu C9920-01 spectrometer with an integral sphere at an excitation wavelength of 320 nm. XRD data for **DMAc-BN** and **PXZ-BN** were collected on a Rigaku Saturn 724 charged-coupled-device (CCD) diffractometer using Mo-*K*α (λ = 0.71075 Å). Single crystals of **DMAc-BN** [$C_{36}H_{29}BN_2$, Mw = 500.45] and **PXZ-BN** [$C_{30}H_{17}BN_2O_2$, Mw = 448.29] suitable for X-ray analysis were grown by slow gradient sublimation. Data collection, cell refinements, and data reductions were conducted using the CrysAlisPro software[2]. The structure was solved by direct methods using the SHELXT[3] program and were refined by full-matrix least-squares methods on F^2 using SHELXL2014[4]. All materials for publication were prepared using the Yadokari-XG 2009 soft-ware[5].

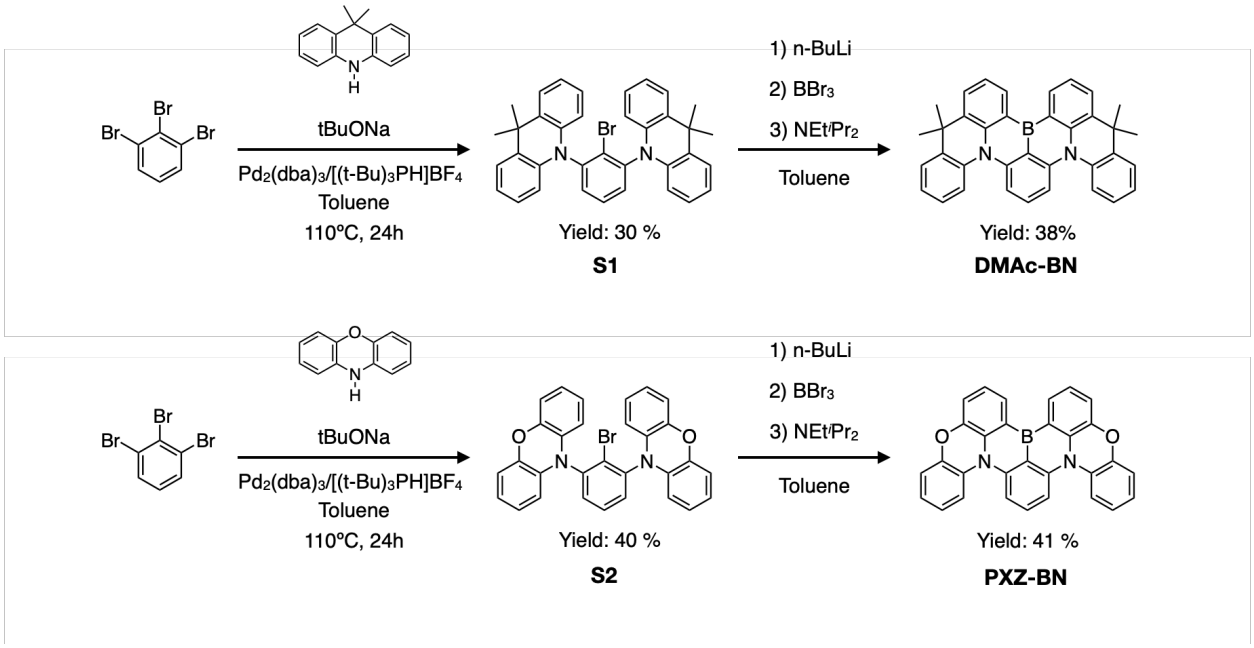

Scheme S1. Synthesis of **DMAc-BN** and **PXZ-BN**.

Synthesis of 10,10'-(2-bromo-1,3-phenylene)bis(9,9-dimethyl-9,10-dihydroacridine) (S1)

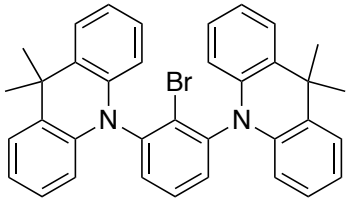

To a 200 mL 4-necked flask, a mixture of toluene solution of 9,9-dimethyl-9,10-dihydroacridine (0.175 g, 0.834 mmol), 1,2,3-tribromobenzene (0.131 g, 0.417 mmol), tBuONa (0.04 g, 0.417 mmol), $Pd_2(dba)_3$ (0.0192 g, 0.021 mmol) and $[(t\text{-}Bu)_3PH]BF_4$ (0.0183 g, 0.063 mmol) were added. The mixture was heated to 110 ºC and stirring 24 hrs. After washing with deionized water three times and extracted with toluene, then dry-over with $MgSO_4$, and evaporated. After drying in vacuum-dry box for 12 hrs. Dark-orange liquid crude product was obtained. After purification of silica gel column chromatography (hexane/toluene = 2/1), 0.072 g of white solid target compound can be obtained, yield 30%. ^{1}H NMR (C_6D_6, 25 ºC, 600 MHz) δ/ppm 7.38 (dd, J = 1.5, 7.7 Hz, 4H), 7.04-7.01 (m, 3H), 6.97 (td, J = 1.6, 6.0, 4H), 6.92 (td, J = 1.1, 6.0 Hz, 4H), 6.43 (dd, J = 1.0, 8.1 Hz, 4H), 1.70 (s, 6H), 1.57 (s, 6H); ^{13}C NMR ($CDCl_3$, 25 ºC, 150 MHz) δ/ppm 143.02, 139.17, 133.82, 131.73, 131.30, 130.12, 126.71, 125.85, 121.18, 113.28, 36.07, 33.12, 31.02; MS: m/z = 570.17 $[M+H]^+$ (ASAP).

Synthesis of (DMAc-BN)

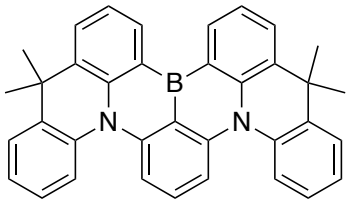

A solution of *n*-butyllithium in hexane (0.664 mL, 1.59 M, 1.056 mmol) was added slowly to a solution of **S1** (0.548 g, 0.96 mmol) in toluene (30 mL) at –50 ºC under a nitrogen atmosphere. After stirring at 60 ºC for 0.5 h, hexane was removed *in vacuo*. After addition of boron tribromide (1.15 mL, 1.15 mmol) at –60 ºC, the reaction mixture was stirred at room temperature for 0.5 h. *N*,*N*-Diisopropylethylamine (0.331 mL, 1.920 mmol) was added at 0 ºC and then the reaction mixture was allowed to warm to room temperature. After stirring at 110 ºC overnight, the reaction mixture was cooled to room temperature. the solvent was removed *in vacuo*. The residue was dissolved in toluene and then filtered with a pad of Florisil® (eluent: toluene). The crude product was washed with hexane, acetonitrile, and toluene by using a sonicator to obtain the title compound (182 mg, yield: 38 %) as a yellow solid. ^{1}H NMR (C_6D_6, 25 ºC, 600 MHz) δ/ppm 8.57 (d, J = 7.4 Hz, 2H), 7.57 (d, J = 8.2 Hz, 2H), 7.55-7.52 (m, 4H), 7.38 (d, J = 7.9 Hz, 2H), 7.33 (t, J = 7.4 Hz,

2H), 7.25 (t, J = 8.2 Hz, 1H), 7.03-7.02 (m, 2H), 6.93 (t, J = 8.0 Hz, 2H), 1.75 (s, 6H), 1.38 (s, 6H). ^{11}B NMR (190 MHz, C_6D_6) δ/ppm 40.63. ^{13}C NMR (150 MHz, C_6D_6) δ/ppm 143.90, 143.43, 140.61, 138.36, 135.25, 132.90, 131.21, 125.99, 125.95, 124.45, 123.92, 122.83, 120.23, 110.14, 37.03, 30.65, 22.73; MS: m/z = 500.24 $[M+H]^+$ (ASAP); Anal calcd for $C_{36}H_{29}BN_2$: C 86.40; H, 5.84; N, 5.60 %. Found: C, 86.62; H, 6.05; N, 5.69 %.

Synthesis of 10,10'-(2-bromo-1,3-phenylene)bis(10H-phenoxazine) (S2)

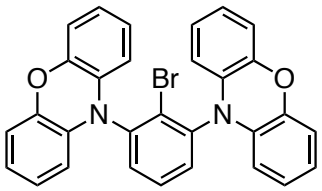

To a 200 mL 4-necked flask, a mixture of toluene solution of 10H-phenoxazine (0.59 g, 3.18 mmol), 1,2,3-tribromobenzene (0.5 g, 1.59 mmol), tBuONa (0.31 g, 3.18 mmol), $Pd_2(dba)_3$ (0.074 g, 0.080 mmol) and $[(t\text{-}Bu)_3PH]BF_4$ (0.070 g, 0.24 mmol) were added. The mixture was heated to 110 ºC and stirring 24 hrs. After washing with deionized water three times and extracted with toluene, then dry-over with $MgSO_4$, and evaporated. After drying in vacuum-dry box for 12 hrs. Dark-orange liquid crude product was obtained. After washing with cooled toluene, 0.33 g of gray solid target compound can be obtained, yield 40%. ^{1}H NMR ($CDCl_3$, 25 ºC, 600 MHz) δ/ppm 7.76 (t, J = 7.6 Hz, 1H), 7.60 (d, J = 7.9 Hz, 2H), 6.74-6.65 (m, 12H), 5.84 (d, J = 7.7 Hz, 4H).^{13}C NMR ($CDCl_3$, 25 ºC, 150 MHz) δ/ppm 143.89, 140.82, 133.90, 132.47, 131.86, 131.37, 123.50, 122.04, 115.92, 112.73; MS: m/z = 518.06 $[M+H]^+$ (ASAP).

Synthesis of (PXZ-BN)

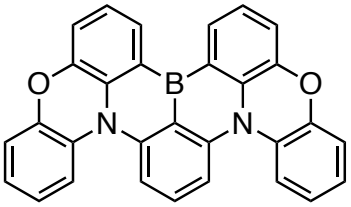

Compound **PXZ-BN** was synthesized according to the same procedure described above for the synthesis of **DMAc-BN**, using **S2** (1.71 g, 3.30 mmol), *n*-BuLi (2.66 M, 1.36 mL, 3.63 mmol), BBr_3 (3.94 mL, 3.96 mmol), $NEt(i\text{-}Pr)_2$ (1.14 mL, 6.60 mmol), yielding **PXZ-BN** as an orange solid (yield = 0.60 g, 41%). ^{1}H NMR (C_6D_6, 25 ºC, 600 MHz) δ/ppm 8.05 (d, J = 7.4 Hz, 2H), 7.42 (t, J = 8.3 Hz, 4H), 7.13-7.11 (m, 3H), 7.04 (d, J = 8.0 Hz, 2H), 6.99 (t, J = 7.6 Hz, 2H), 6.75 (t, J = 8.5 Hz, 2H), 6.66 (t, J = 8.1 Hz, 2H). ^{11}B NMR (190 MHz, C_6D_6) δ/ppm 41.56. ^{13}C NMR (150

MHz, C_6D_6) δ/ppm 149.72, 147.49, 141.40, 137.12, 131.51, 131.11, 128.60, 125.23, 123.26, 123.15, 118.68, 117.65, 117.31, 107.94; MS: m/z = 448.14 $[M+H]^+$ (ASAP); Anal calcd for $C_{30}H_{17}BN_2O_2$: C 80.38; H, 3.82; N, 6.25 %. Found: C, 80.42; H, 3.87; N, 6.30 %.

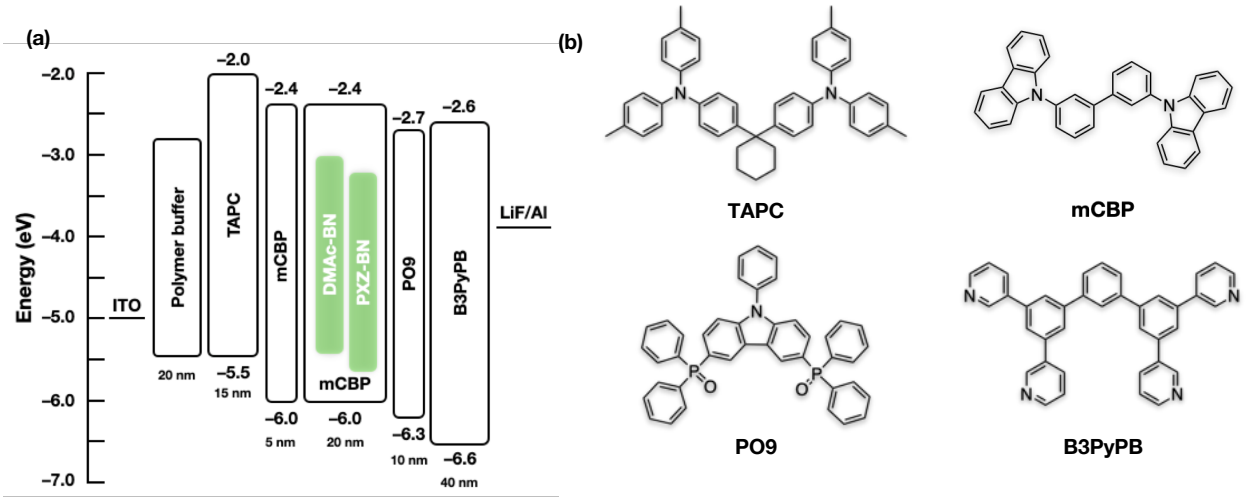

Figure S1. (a) Energy level diagram of OLEDs based on **DMAc-BN** and **PXZ-BN** and (b) molecular structures of used materials.

Table S1. OLED characteristics employing **DMAc-BN** and **PXZ-BN** as an emitter.

	λ_{EL} [a] (nm)	FWHM [b] (nm)	CIE [c] (x, y)	$CE_{MAX}/CE_{100}/CE_{1000}$ [d] (cd/A)	$PE_{MAX}/PE_{100}/PE_{1000}$ [e] (lm/W)	$EQE_{MAX}/EQE_{100}/EQE_{1000}$ [f] (%)
DMAc-BN	**503**	**49**	**0.18, 0.60**	**57.0/49.7/34.2**	**49.7/26.6/20.1**	**20.3/17.6/12.0**
PXZ-BN	**516**	**47**	**0.22, 0.67**	**83.8/71.4/40.9**	**70.1/50.0/22.1**	**23.3/19.9/11.3**

a) Emission maximum. b) Full width at half maximum. c) CIE coordinates. d) Current efficiency: maximum, value at 100 and 1000 cd m^{-2}. e) Power efficiency: maximum, value at 100 and 1000 cd m^{-2}. f) External quantum efficiency: maximum, value at 100 and 1000 cd m^{-2}.

Estimation of the rate constants. Rate constants were determined from the measurements of quantum yields and lifetimes of the fluorescence and TADF components according to the equations 1-7[6].

Φ_{PL}	0.88		
Φ_F	0.81		
Φ_{TADF}	0.07		
τ_{PF}	6.2 ns		
τ_{DF}	32.9 µs		
k_F	13.065 X 10^7 s^{-1}	$k_F = \Phi_F/\tau_{PF}$	(1)
k_{IC}	1.7815 X 10^7 s^{-1}	$\Phi_{PL} = k_F/(k_F + k_{IC})$	(2)
k_{ISC}	1.2830 X 10^7 s^{-1}	$\Phi_F = k_F/(k_F + k_{IC} + k_{ISC})$	(3)
Φ_{IC}	0.11045	$\Phi_{IC} = k_{IC}/(k_F + k_{IC} + k_{ISC})$	(4)
Φ_{ISC}	0.079545	$\Phi_{ISC} = 1 - \Phi_F - \Phi_{IC} = k_{ISC}/(k_F + k_{IC} + k_{ISC})$	(5)
k_{DF}	2.67 X 10^4 s^{-1}	$k_{DF} = \Phi_{TADF}/\Phi_{ISC}\tau_{DF}$	(6)
k_{RISC}	2.35 X 10^4 s^{-1}	$k_{RISC} = k_F k_{DF} \Phi_{TADF}/k_{ISC}\Phi_F$	(7)

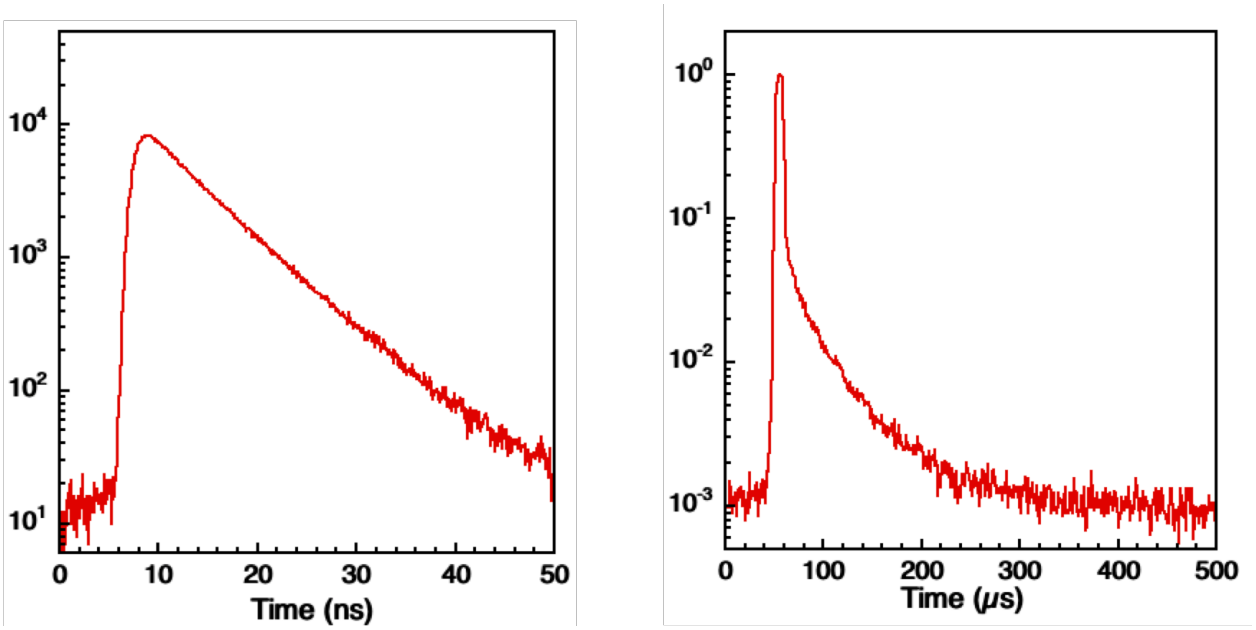

Figure S2. Transient decay spectra of **DMAc-BN** (3 wt% doped in **mCBP** film).

Φ_{PL}	0.90		
Φ_F	0.67		
Φ_{TADF}	0.23		
τ_{PF}	8.2 ns		
τ_{DF}	90.7 μs		
k_F	8.1707 X 10^7 s^{-1}	$k_F = \Phi_F/\tau_{PF}$	(1)
k_{IC}	0.90786 X 10^7 s^{-1}	$\Phi_{PL} = k_F/(k_F + k_{IC})$	(2)
k_{ISC}	3.1165 X 10^7 s^{-1}	$\Phi_\Phi = k_F/(k_F + k_{IC} + k_{ISC})$	(3)
Φ_{IC}	0.074444	$\Phi_{IC} = k_{IC}/(k_F + k_{IC} + k_{ISC})$	(4)
Φ_{ISC}	0.25556	$\Phi_{ISC} = 1 - \Phi_F - \Phi_{IC} = k_{ISC}/(k_F + k_{IC} + k_{ISC})$	(5)
k_{DF}	0.99 X 10^4 s^{-1}	$k_{DF} = \Phi_{TADF}/\Phi_{ISC}\tau_{DF}$	(6)
k_{RISC}	0.89 X 10^4 s^{-1}	$k_{RISC} = k_F k_{DF} \Phi_{TADF}/k_{ISC}\Phi_F$	(7)

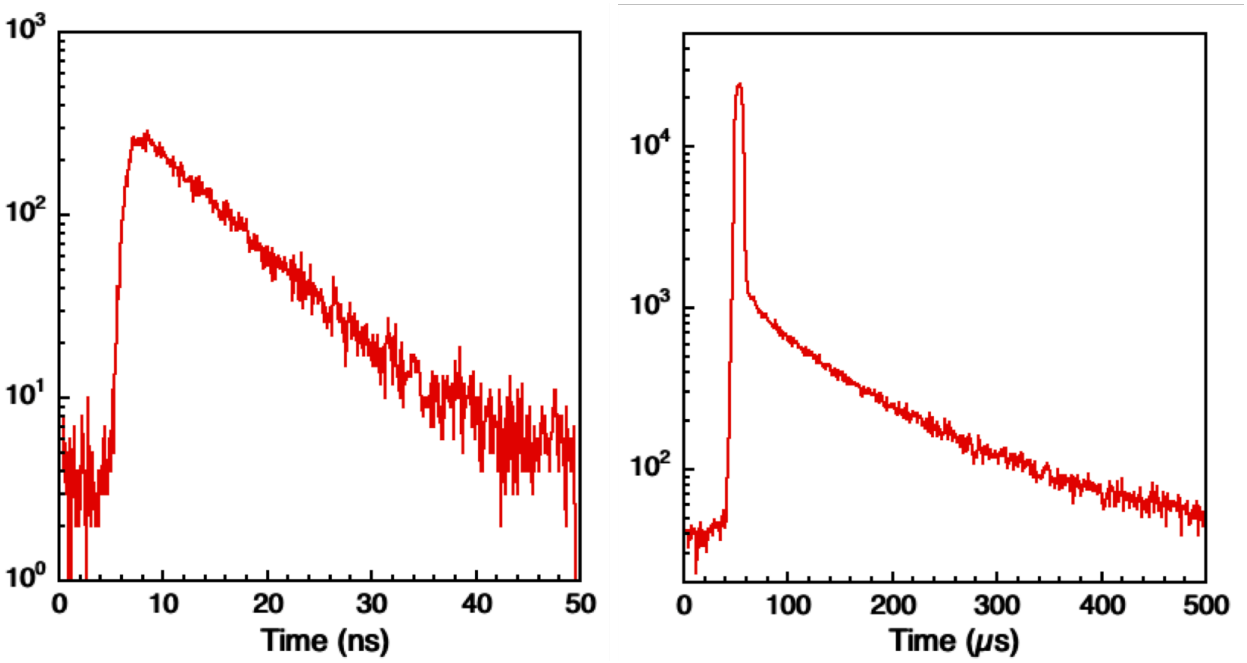

Figure S3. Transient decay spectra of **PXZ-BN** (3 wt% doped in **mCBP** film).

Table S2. Crystallography data for **DMAc-BN** and **PXZ-BN**

Compound	**DMAc-BN**	**PXZ-BN**
Chemical formula	$C_{36}H_{29}BN_2$	$C_{30}H_{17}BN_2O_2$
Formula weight	500.42	448.26
Temperature (K)	150	150
Radiation type	Mo *Kα*	Mo *Kα*
Wavelength (Å)	0.71073	0.71073
Crystal system	Monoclinic	Monoclinic
Space group	$P2_1/c$	$P2_1/c$
a (Å)	15.4909(12)	13.2859(5)
b (Å)	12.5886(6)	19.1633(7)
c (Å)	15.0722(12)	8.0760(3)
α (°)	90	90
β (°)	180.225(10)	98.084(3)
γ (°)	90	90
Volume (Å^3)	2589.7(4)	2035.73(13)
Z	4	4
Density (calculated) (g/cm^3)	1.283	1.463
Absorption coefficient (mm^{-1})	0.074	0.092
F(000)	1056	928
Crystal size (mm^3)	0.250 × 0.150 × 0.100	0.100 × 0.050 × 0.050
Theta range for data collection (°)	2.985 to 27.499	2.630 to 27.496
Index ranges	$-20 \le h \le 20$ $-16 \le k \le 16$ $-19 \le l \le 19$	$-17 \le h \le 17$ $-24 \le k \le 24$ $-10 \le l \le 10$
Reflections collected	35660	28117
Independent reflections	5945 [R(int) = 0.0878]	4684 [R(int) = 0.0555]
Completeness (%)	99.9 (θ = 25.242°)	99.9 (θ = 25.242°)
Absorption correction	Semi-empirical from equivalents	Semi-empirical from equivalents
Maximum and minimum transmission	1.00000 and 0.96230	1.00000 and 0.77991
Refinement method	Full-matrix least-squares on F^2	Full-matrix least-squares on F^2
Data/restraints/parameters	5945 / 0 / 356	4684 / 0 / 316
Goodness-of-fit on F^2	1.028	1.032
Final *R* indices [$I > 2\sigma(I)$]	R_1 = 0.0522, wR_2 = 0.1125	R_1 = 0.0400, wR_2 = 0.0893
R indices (all data)	R_1 = 0.0956, wR_2 = 0.1329	R_1 = 0.0598, wR_2 = 0.0972
Largest diff. peak and hole (e·Å^{-3})	0.212 and −0.202	0.251 and −0.199

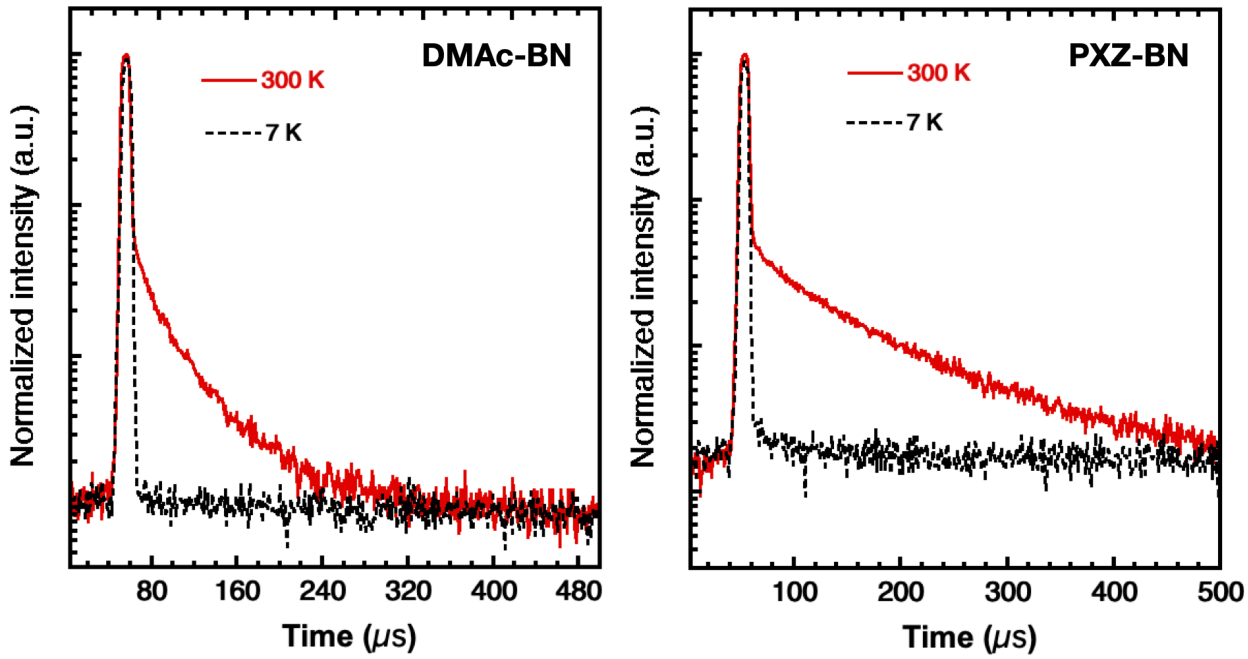

Figure S4. Transient PL decay curves of **DMAc-BN** and **PXZ-BN** in 3 wt%-doped films with **mCBP** host at 7K and 300K, respectively.

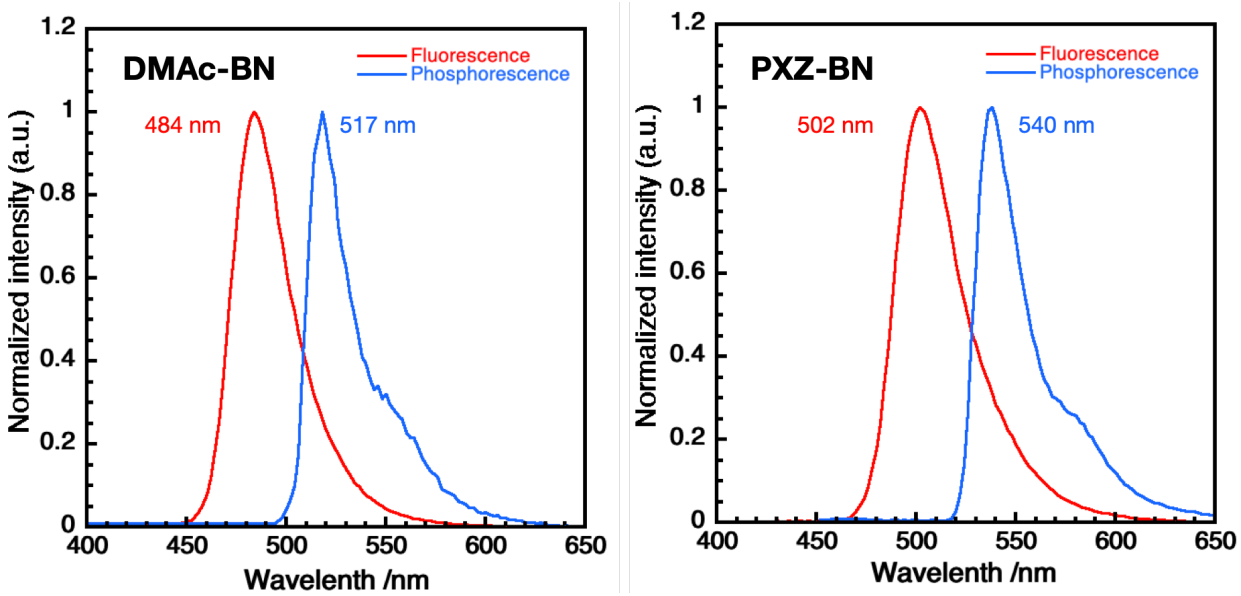

Figure S5. Fluorescence (300K) and phosphorescence (77K) spectra of **DMAc-BN** and **PXZ-BN** in 2-MeTHF solutions (2 X 10^{-5} M).

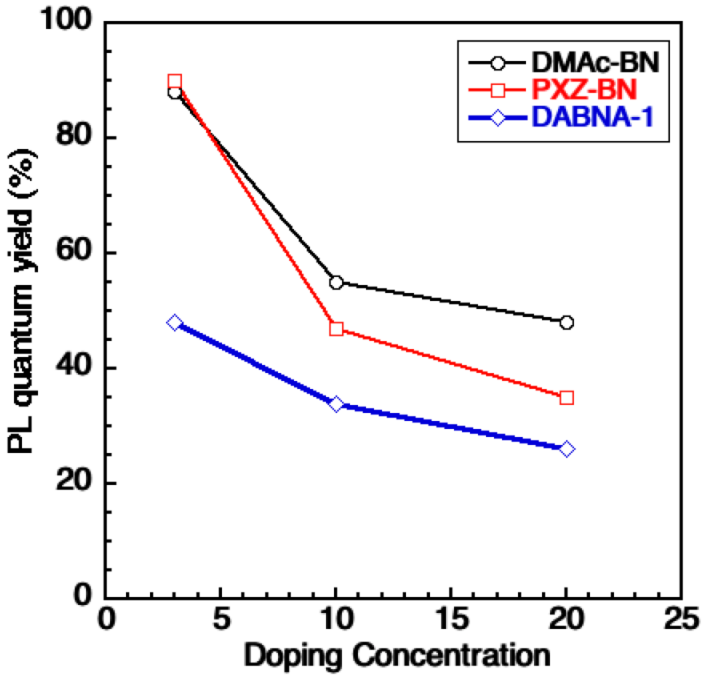

Figure S6. PLQYs of **DMAc-BN**, **PXZ-BN** and **DABNA-1** doped **mCBP** films.

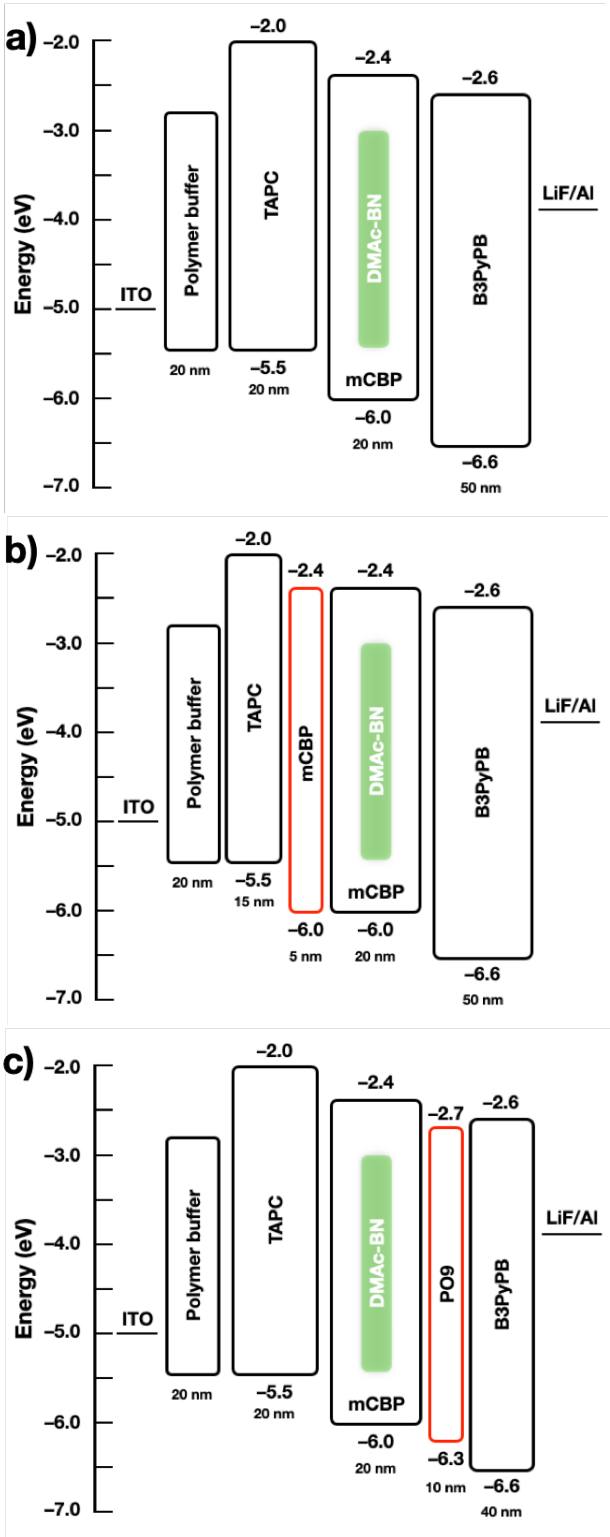

Figure S7. Energy level diagrams of OLEDs using 3wt % **DMAc-BN**/mCBP film as the emission layer. a) Device A without using both mCBP and PO9, b) Device B using mCBP, and c) Device C using PO9.

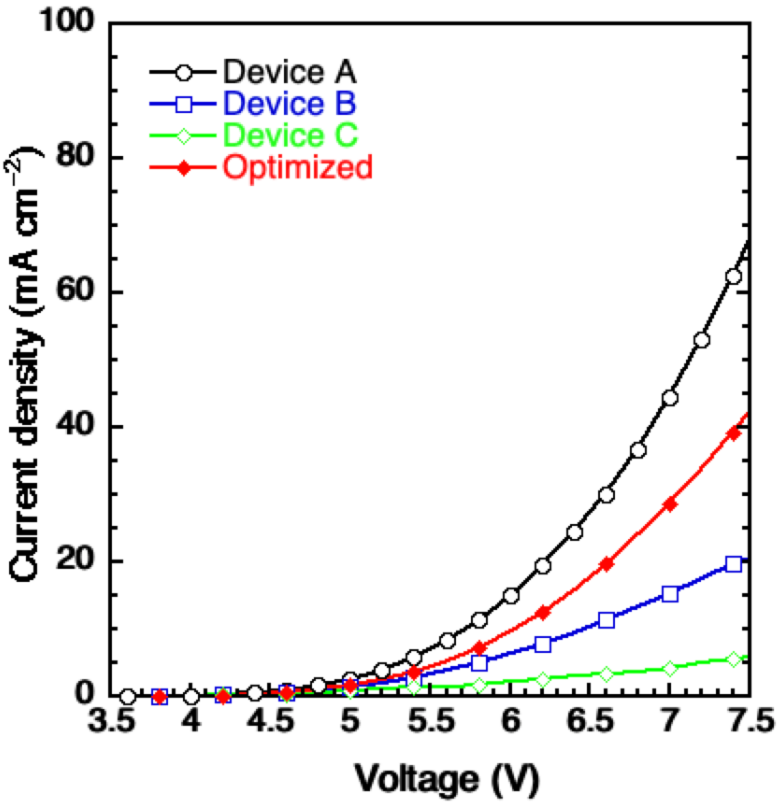

Figure S8. Current density-voltage characteristics of Device A–C, and optimized device reported in the main text.

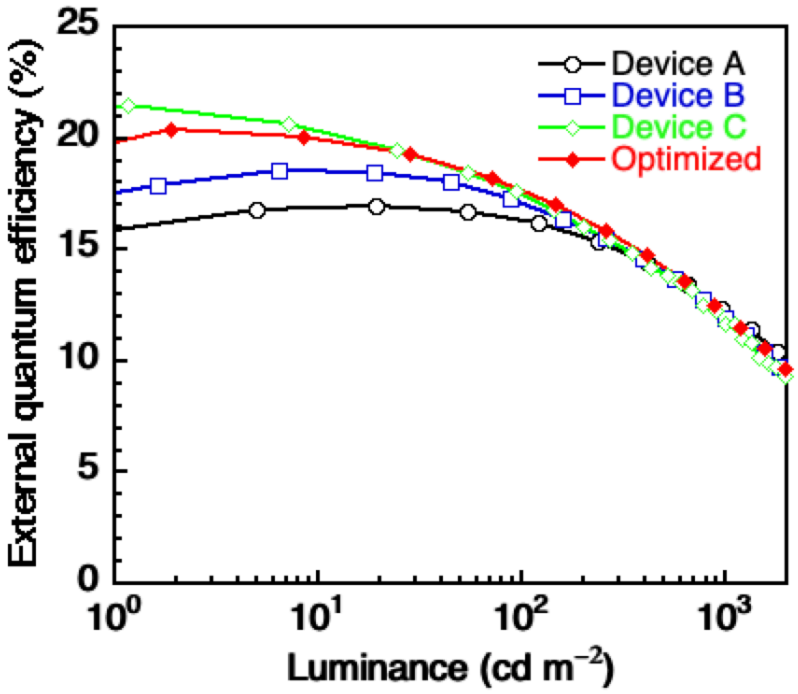

Figure S9. EQE-Luminance characteristics of Device A-C, and optimized device reported in the main text.

Table S2. OLED characteristics of Device A-C, and optimized device.

	λ_{EL}[a] (nm)	FWHM[b] (nm)	CIE[c] (x, y)	$CE_{MAX}/CE_{100}/CE_{1000}$[d] (cd/A)	$PE_{MAX}/PE_{100}/PE_{1000}$[e] (lm/W)	$EQE_{MAX}/EQE_{100}/EQE_{1000}$[f] (%)
Device A	**505**	**49**	**0.18, 0.60**	**52.4/50.4/38.1**	**46.4/37.9/23.7**	**17.8/17.2/12.9**
Device B	**506**	**49**	**0.18, 0.60**	**56.9/51.0/37.0**	**50.3/35.2/18.4**	**18.9/17.0/12.3**
Device C	**506**	**49**	**0.16,0.61**	**63.1/51.4/34.2**	**58.3/38.2/16.8**	**21.5/17.5/11.6**
Optimized	**503**	**49**	**0.18, 0.60**	**57.0/49.7/34.2**	**49.7/26.6/20.1**	**20.3/17.6/12.0**

a) Emission maximum. b) Full width at half maximum. c) CIE coordinates. d) Current efficiency: maximum, value at 100 and 1000 cd m^{-2}. e) Power efficiency: maximum, value at 100 and 1000 cd m^{-2}. f) External quantum efficiency: maximum, value at 100 and 1000 cd m^{-2}.

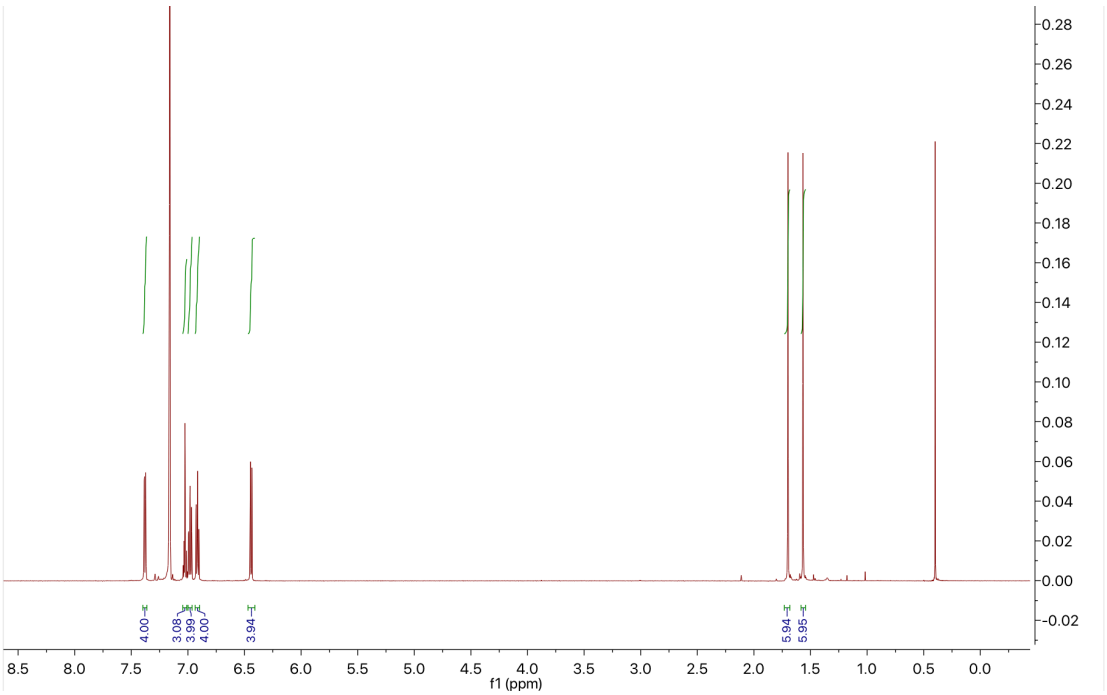

Figure S10. ^{1}H NMR of **S1** (C_6D_6, 25 ºC, 600 MHz).

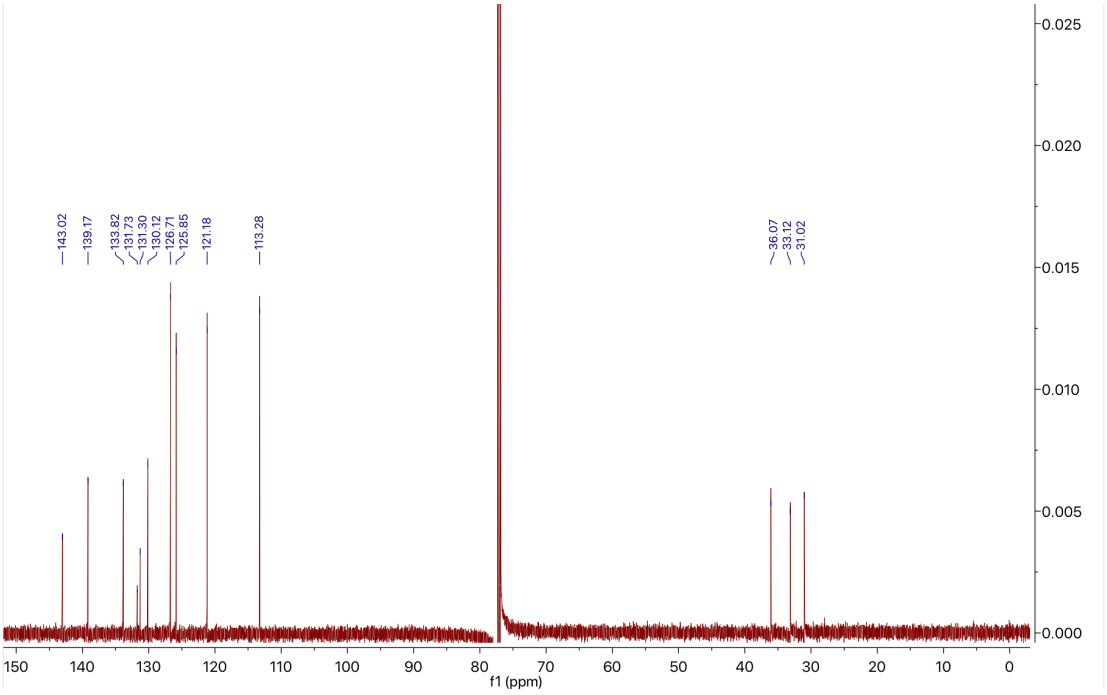

Figure S11. ^{13}C NMR of **S1** ($CDCl_3$, 25 ºC, 150 MHz).

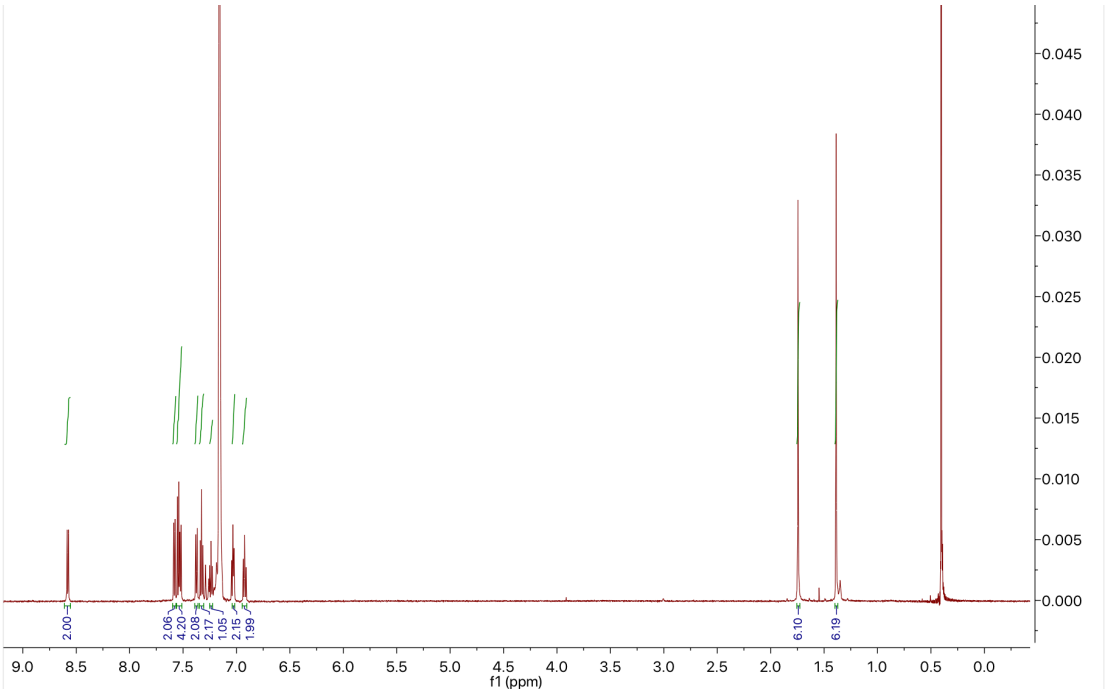

Figure S12. ^{1}H NMR of **DMAc-BN** (C_6D_6, 25 ºC, 600 MHz).

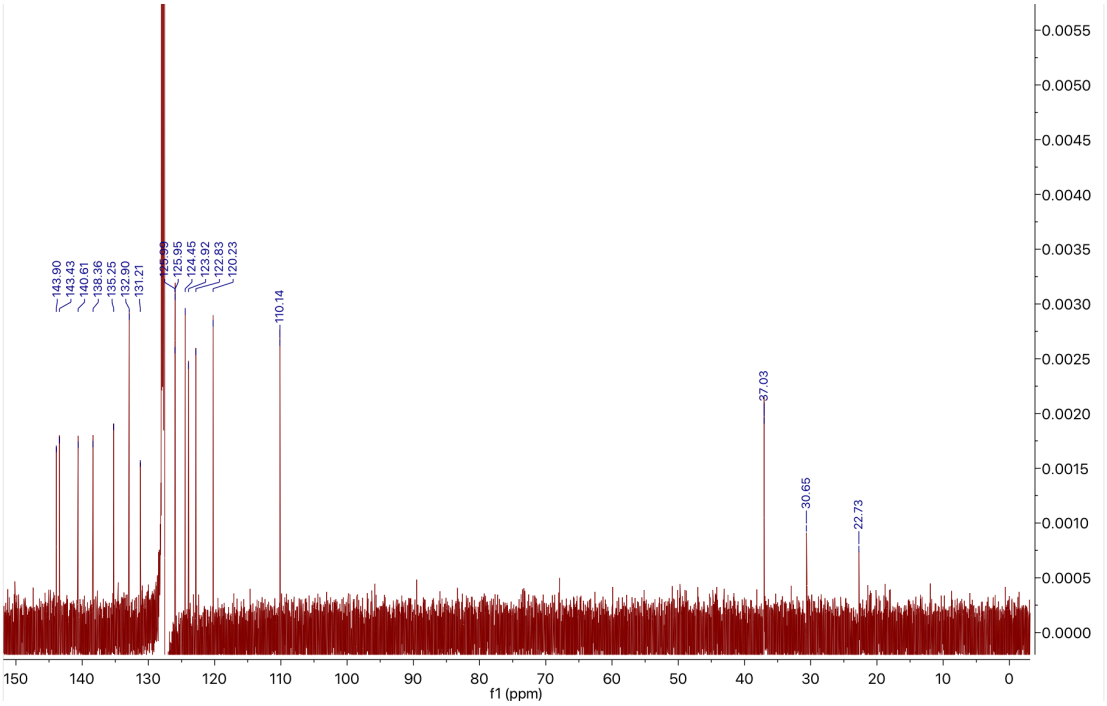

Figure S13. ^{13}C NMR of **DMAc-BN** (C_6D_6, 25 ºC, 150 MHz).

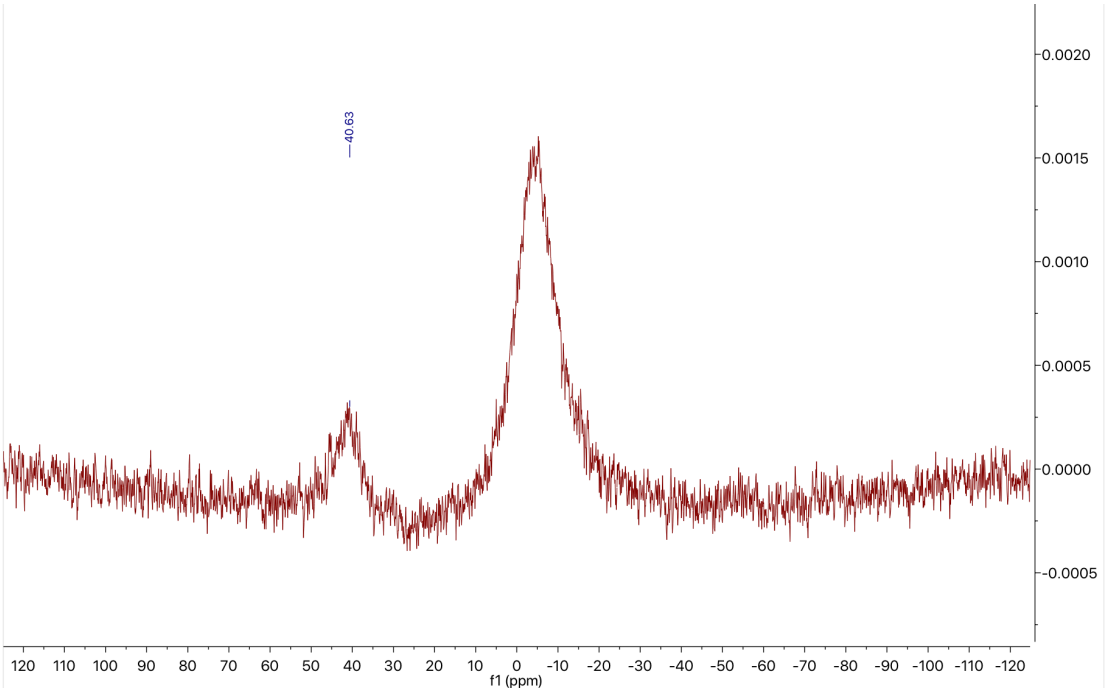

Figure S14. ^{11}B NMR of **DMAc-BN** (C_6D_6, 25 ºC, 190 MHz).

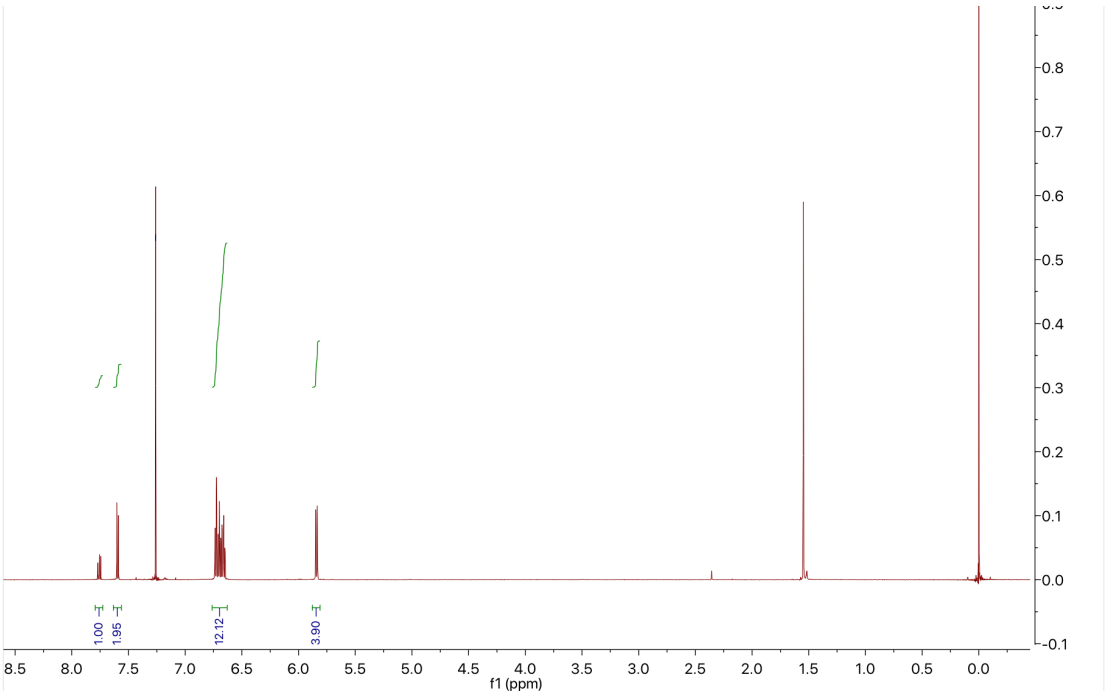

Figure S15. ^{1}H NMR of **S2** ($CDCl_3$, 25 ºC, 600 MHz).

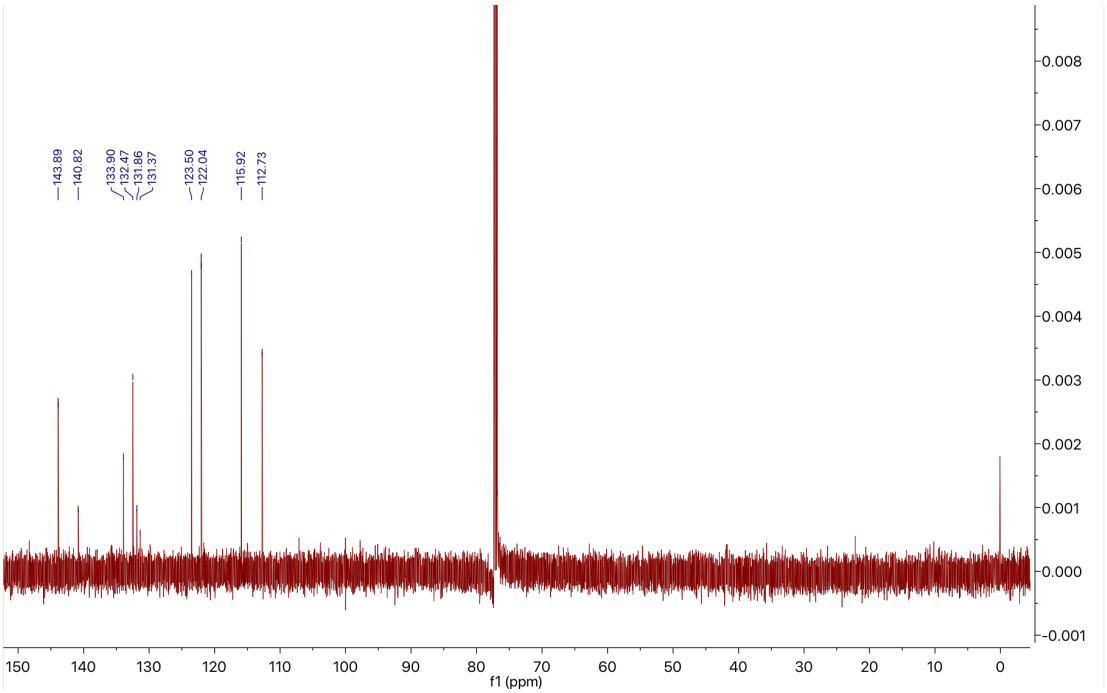

Figure S16. ^{13}C NMR of **S2** ($CDCl_3$, 25 ºC, 150 MHz).

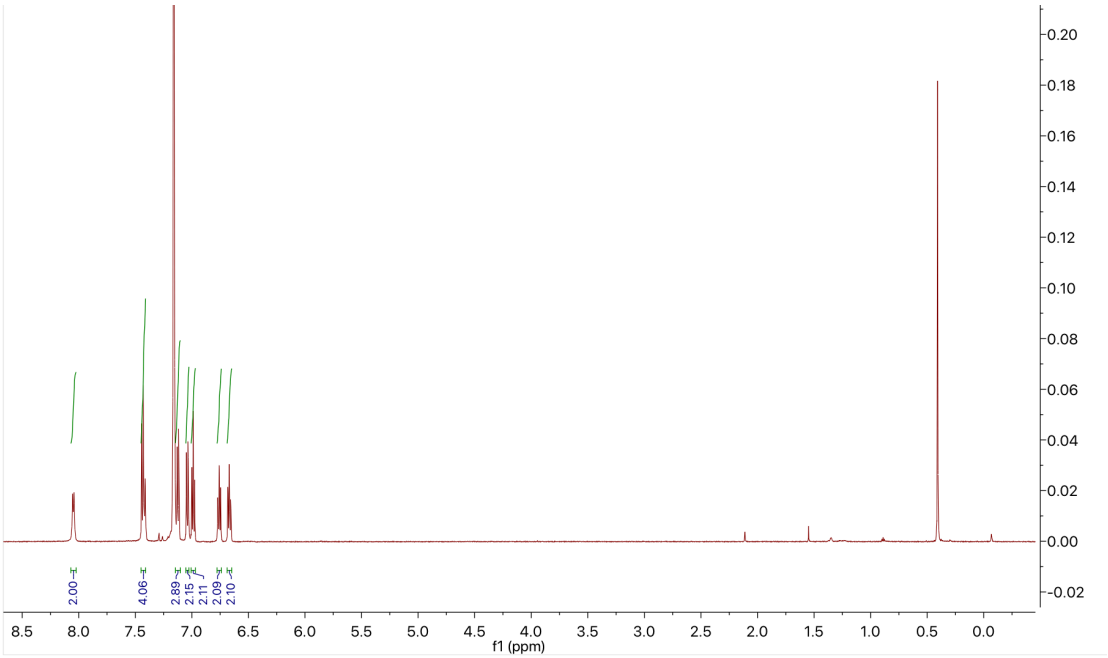

Figure S17. ^{1}H NMR of **PXZ-BN** (C_6D_6, 25 ºC, 600 MHz).

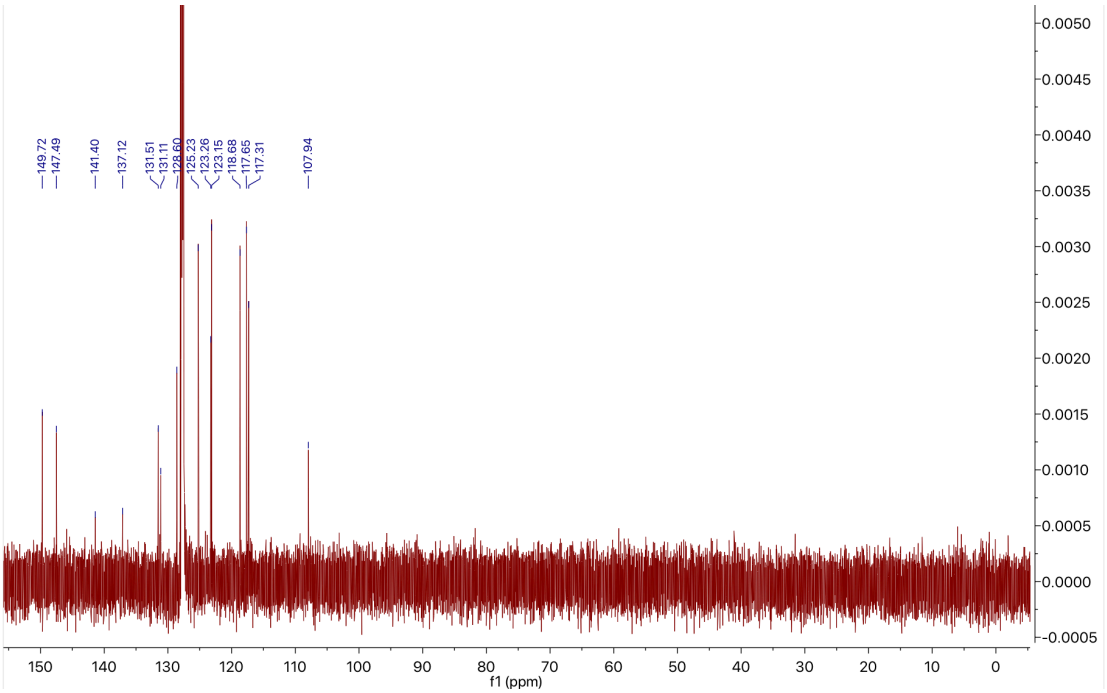

Figure S18. ^{13}C NMR of **PXZ-BN** (C_6D_6, 25 ºC, 150 MHz).

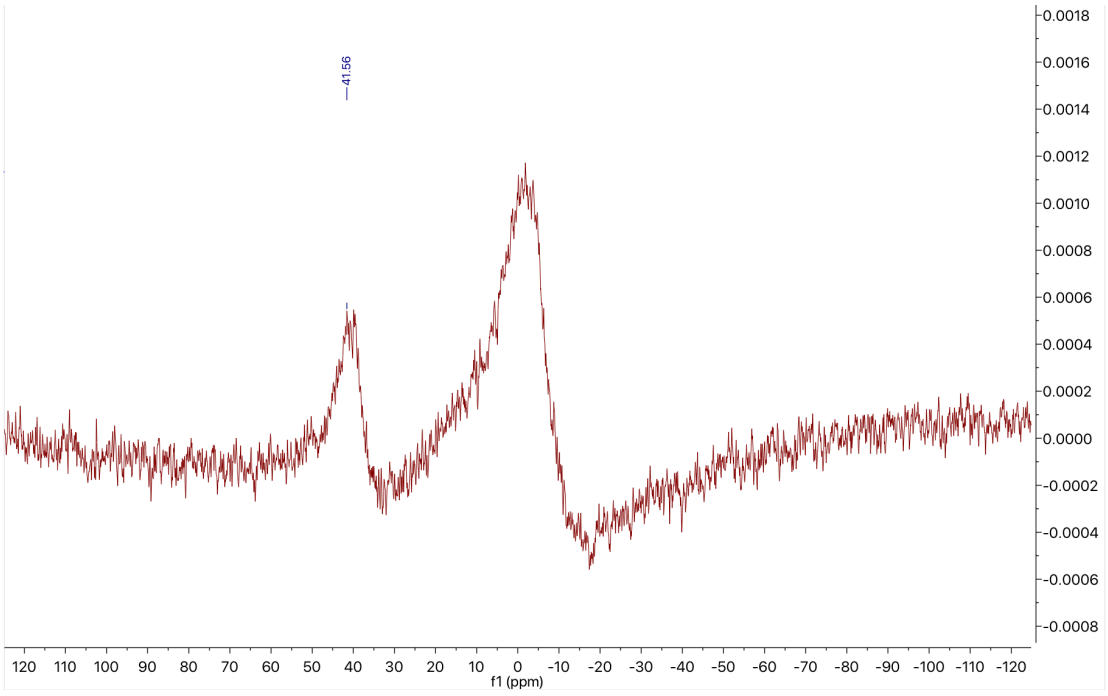

Figure S19. ^{11}B NMR of **PXZ-BN** (C_6D_6, 25 ºC, 190 MHz).

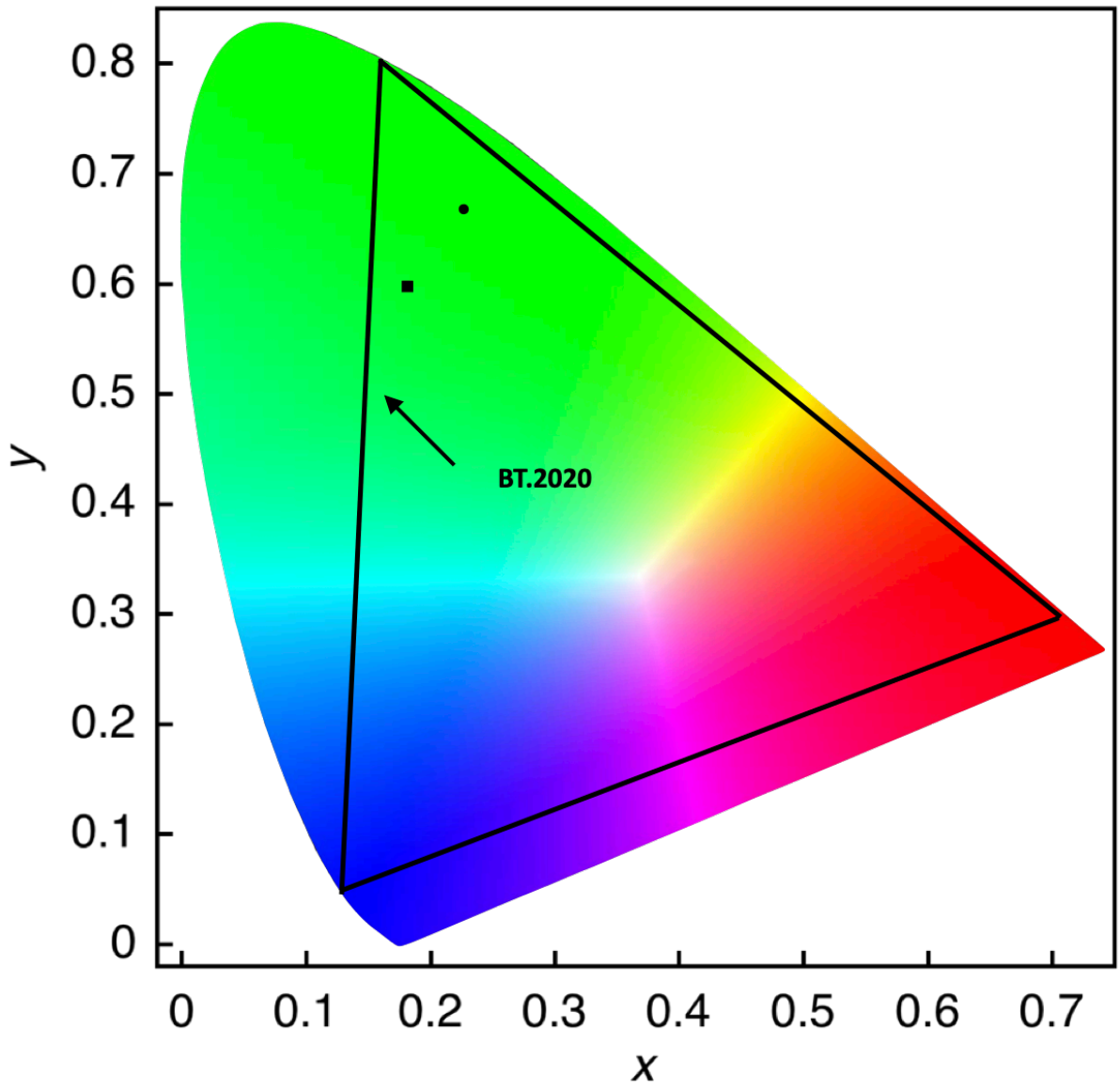

Figure S20. CIE (x,y) coordinates of **DMAc-BN** (0.18, 0.60) and **PXZ-BN** (0.22, 0.67).

Reference:

(1) *Gaussian 09*, Revision D.01, M. J. Frisch, G. W. Trucks, H. B. Schlegel, G. E. Scuseria, M. A. Robb, J. R. Cheeseman, G. Scalmani, V. Barone, B. Mennucci, G. A. Petersson, H. Nakatsuji, M. Caricato, X. Li, H. P. Hratchian, A. F. Izmaylov, J. Bloino, G. Zheng, J. L. Sonnenberg, M. Hada, M. Ehara, K. Toyota, R. Fukuda, J. Hasegawa, M. Ishida, T. Nakajima, Y. Honda, O. Kitao, H. Nakai, T. Vreven, J. A. Montgomery, Jr., J. E. Peralta, F. Ogliaro, M. Bearpark, J. J. Heyd, E. Brothers, K. N. Kudin, V. N. Staroverov, R. Kobayashi, J. Normand, K. Raghavachari, A. Rendell, J. C. Burant, S. S. Iyengar, J. Tomasi, M. Cossi, N. Rega, J. M. Millam, M. Klene, J. E. Knox, J. B. Cross, V. Bakken, C. Adamo, J. Jaramillo, R. Gomperts, R. E. Stratmann, O. Yazyev, A. J. Austin, R. Cammi, C. Pomelli, J. W. Ochterski, R. L. Martin, K. Morokuma, V. G. Zakrzewski, G. A. Voth, P. Salvador, J. J. Dannenberg, S. Dapprich, A. D. Daniels, Ö. Farkas, J. B. Foresman, J. V. Ortiz, J. Cioslowski, and D. J. Fox, Gaussian, Inc., Wallingford CT, 2013.
(2) *CrysAlisPro CCD, CrysAlisPro RED and ABSPACK in CrysAlisPro RED*; Oxford Diffraction Ltd.: Abingdon, England, 2006.
(3) Sheldrick, G. M. SHELXT – Integrated Space-Group and Crystal-Structure Determination. *Acta Crystallogr., Sect. A: Found. Adv.* **2015**, *71*, 3–8.
(4) Sheldrick, G. M. Crystal Structure Refinement with SHELXL. *Acta Crystallogr., Sect. C: Cryst. Struct. Commun.* **2015**, *71*, 3–8.
(5) Kabuto, C.; Akine, S.; Nemoto, T.; Kwon, E. Release of Software (Yadokari-XG 2009) for Crystal Structure Analyses. *Nihon Kessho Gakkaishi* **2010**, *51*, 218–224.
(6) Masui, K., Nakanotani, H. & Adachi, C. *Org. Electron.* **14**, 2721-2726 (2013).